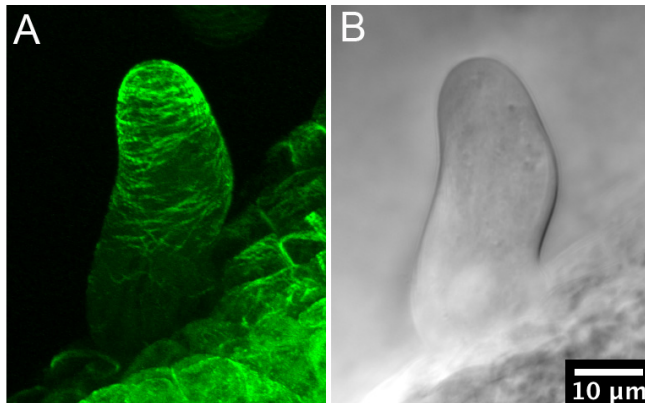
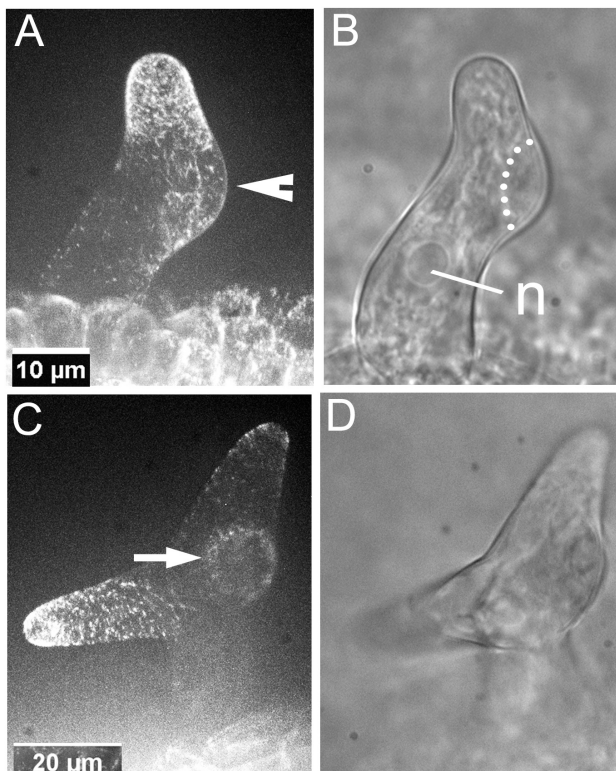


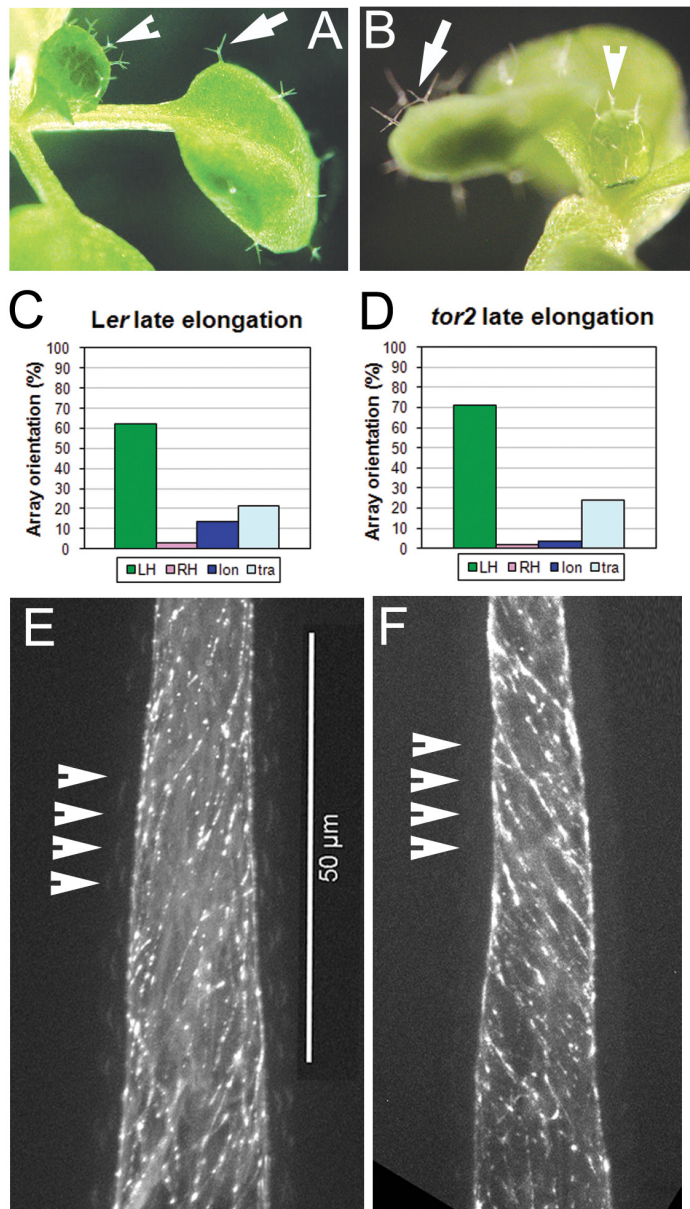
Supplemental Figures



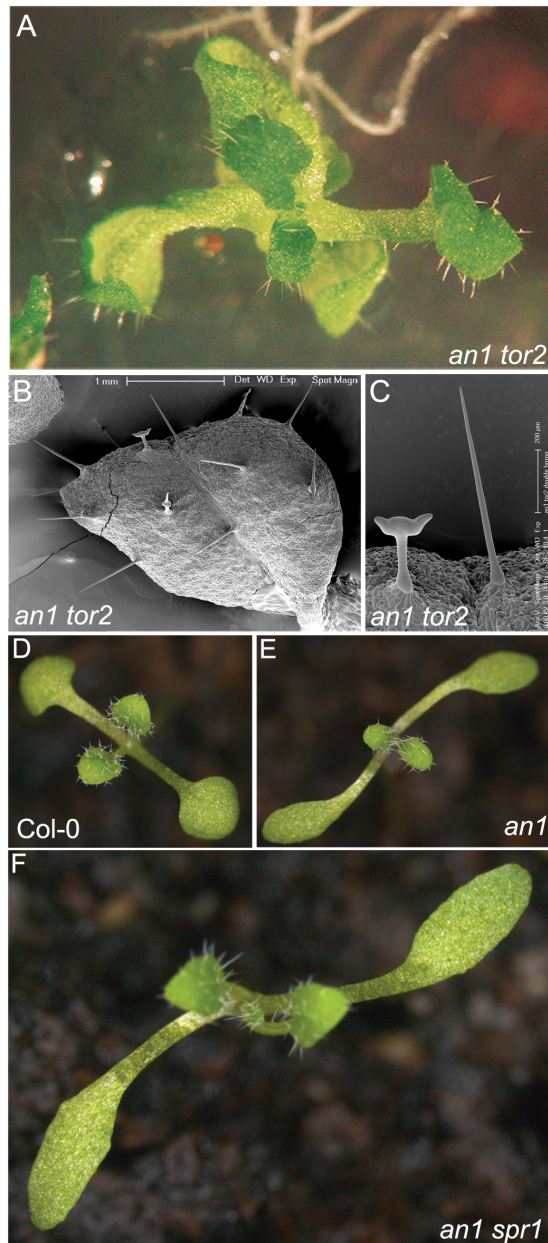
Supplemental Figure 1. The GFP-TUB6 line suggests that in trichome branching the formation of the early bulge occurs without specific cortical microtubule accumulations. (A) Wild-type trichome of a plant expressing GFP-TUB6. Note strong microtubule signal in the apical collar. A gentle bulge below the collar indicated that the trichome shown was undergoing branch formation. (B) Transmission photograph of the same trichome. Scale bar 10 μm .



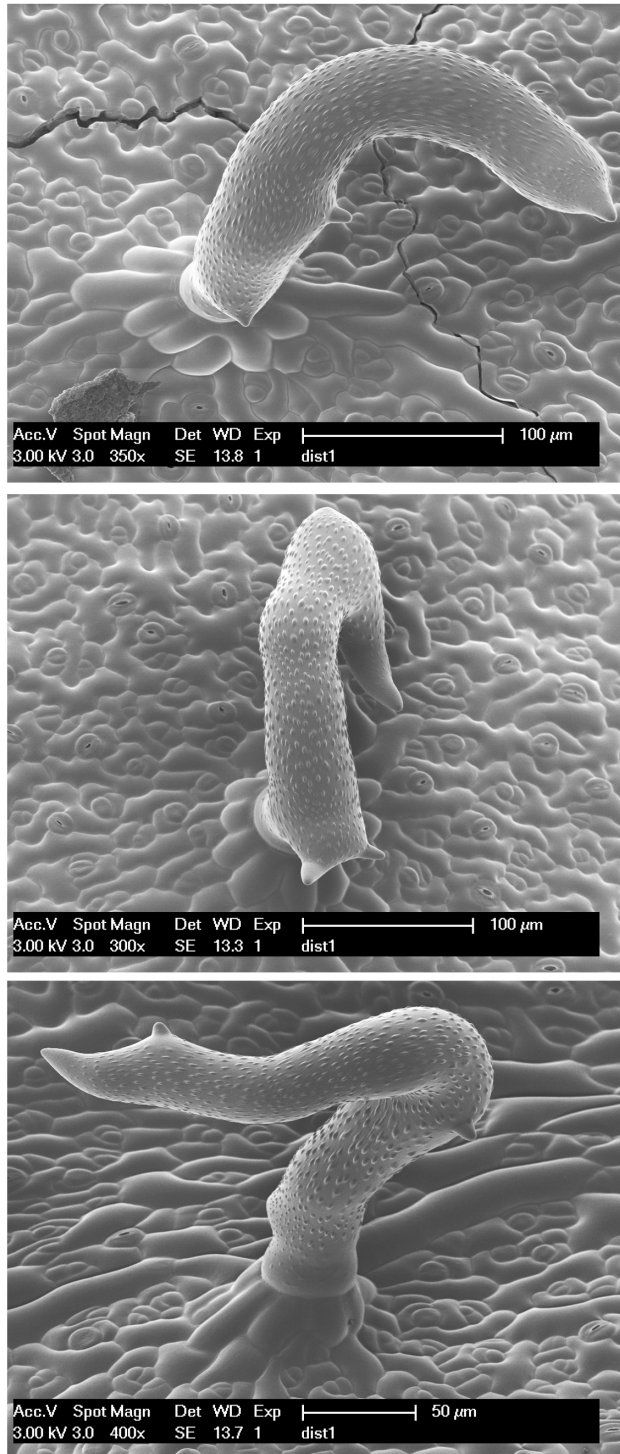
Supplemental Figure 2. EB1-GFP visualizes a wide ring of microtubules formed on early bulging trichome branches. (A) and (B) primary branching. (A) The projected z-scan shows a wide microtubule free zone in the centre of the bud (arrowhead). A faint ring of EB1-labelled microtubules outlines the bud. (B) Transmission picture of the same trichome. The positions of the microtubule ring and the nucleus (n) are indicated. (C) and (D) secondary branching. (C) The projected z-scan shows a ring of EB1-labelling marking the edge of the bud, which has a microtubule-free zone in its centre. (D) Transmission picture of trichome in (C).



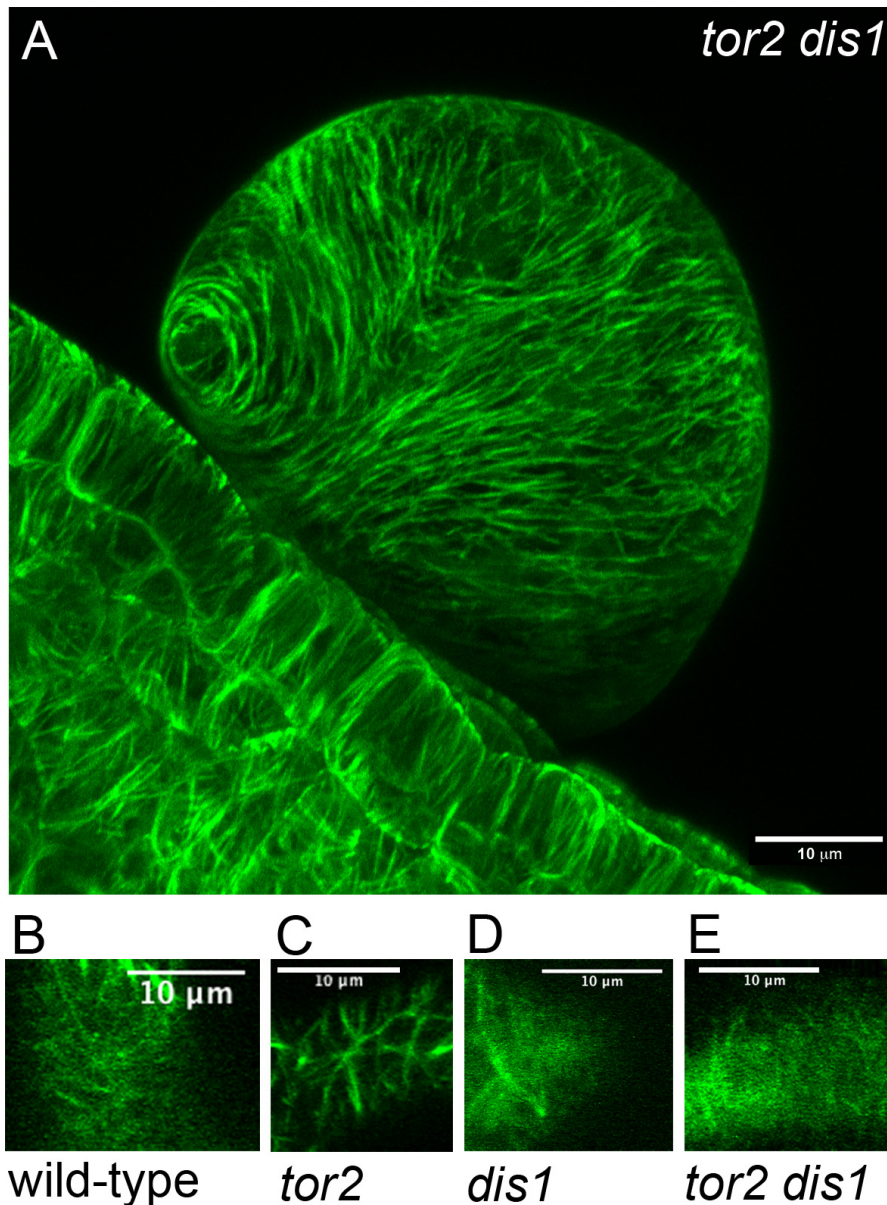
Supplemental Figure 3. Assessment of microtubule orientation in late growing and fully grown trichomes using various microtubule markers. (A, B) Selection of late growing trichomes on 11 to 12 day old plants using a dissecting microscope. Arrowheads indicate smaller, immature trichomes, arrows indicate the larger, more mature trichomes seen on leaves generated by the previous plastochron. The leaves exhibiting younger trichomes showed branches $> 75 \mu\text{m}$ and these were measured and classified as “late elongation”. (A) wild-type *Ler* and (B) *tor2* expressing the GFP-TUB6 marker. (C, D) The leaves selected in (A) and (B) were used for the quantitative analysis of microtubule array orientation in late elongating branches of wild-type and *tor2*. (C) wild-type ($n=66$) and (D) *tor2* ($n=62$). (E, F) Microtubule orientation in branches of non-growing trichomes. Trichomes stem from the second pair of true leaves at 18 days after germination. (E) wild-type (F) *tor2*. Microtubules were visualized using EB1-GFP as a marker (the TUB6-GFP marker produces strong cytoplasmic signals at this stage). Arrowheads show outer cell wall surface, indicative of secondary cell wall thickening seen at this stage. Scale bars (E, F) $50 \mu\text{m}$.



Supplemental Figure 4. Details on *an1 tor2* and *an1 spr1* double mutants. (A) Leaf twisting in *an1 tor2* plants. (B) Overview of an *an1 tor2* leaf showing mainly unbranched, but also few single-branched trichomes. (C) Close-up on *an1 tor2* trichomes. (D) *Col-0* seedling with straight petioles. (E) *an1* seedling (Salk 026489) with cotyledon petioles showing a left-handed twist. (F) The right-handed *spiral1* (*spr1*) mutation is epistatic to *an1* and produces a right-handed twist in the double mutant.



Supplemental Figure 5 Phenotype of *dis1* trichomes in the scanning electron microscope. Three *dis1* mutant trichomes are shown. Cuticular papillae served as landmarks to analyze the growth pattern.



Supplemental Figure 6. Additional examples for an aberrant cytoskeleton in *tor2 dis1* and respective single mutants. (A) An expanding *tor2 dis1* trichome showing mainly isotropic growth. Microtubules are visualized by GFP-TUB6. Note largely parallel microtubule array. (B-E) A comparison of cortical F-actin organization in trichomes of *tor2 dis1* double and respective single mutants. F-actin is visualized by GFP-fABD2. Projections of two to three z-levels (1.3 µm steps) obtained from the trichome's flank are shown. Trichome tips were excluded from the analysis. (B) wild-type, (C) *tor2*, (D) *dis1*, (E) *tor2 dis1*. All bars are 10 µm.